

TWENTY FIRST EUROPEAN ROTORCRAFT FORUM

Paper No. II-14

**THREE-DIMENSIONAL BOUNDARY LAYER PROFILES
ON A MODEL ROTOR**

C. Swales, M.V. Lowson

**DEPARTMENT OF AEROSPACE ENGINEERING
UNIVERSITY OF BRISTOL
ENGLAND**

**August 30 - September 1, 1995
SAINT-PETERSBURG, RUSSIA**

Paper nr.: II.14

Three-Dimensional Boundary Layer Profiles on a Model Rotor.

C. Swales; M.V. Lawson

TWENTY FIRST EUROPEAN ROTORCRAFT FORUM

August 30 - September 1, 1995 Saint-Petersburg, Russia

THREE-DIMENSIONAL BOUNDARY LAYER PROFILES ON A MODEL ROTOR

Swales, C., Lawson, M.V.

Department of Aerospace Engineering
University of Bristol
Bristol
England

Abstract

Helicopter rotor aerodynamics would benefit greatly from the improved understanding which 3D boundary layer velocity information could offer. Hot-wire anemometers and pitot probes are, however, unsuitable as they are intrusive. The Laser Doppler Anemometer (LDA), though non-intrusive, has to date suffered from excessive flare and poor spatial resolution. In this respect this paper describes how improvements in the operation of a three component LDA have led to a unique series of boundary layer velocity profiles being determined on a helicopter rotor operating in hover, revealing data to within 50 microns of the blade surface. These results have provided evidence of the existence of strong radial flows (up to 10% of the chordwise flow) within laminar separation bubbles. The techniques described would be appropriate for any rotating machinery, opening up a whole new area of research.

Introduction

The motivation behind this study was the realisation by Himmelskamp in the 1940s (Ref. 1) that on a rotating propeller blade significantly higher lift coefficients could be maintained near the root than on an equivalent blade mounted statically (3.2 as opposed to 1.4). The postulate is that these high lift coefficients are due to strong spanwise flows within the boundary layer which effectively keep the boundary layer thin, thus inhibiting the onset of stall. Although of profound importance there were various uncertainties relating to the results obtained. In particular it was felt that the results were adversely affected by the large hub and the small aspect ratio of the blades. There has since been considerable discussion regarding enhanced lift near the root but the conclusions have generally been unclear.

In the past any information regarding the state of the boundary layer on rotors has been derived principally from flow visualisation studies. These techniques generally either reveal the surface, or limiting, streamlines, or show the state of the boundary layer, that is whether it is laminar, turbulent, or separated. The techniques however reveal little as to the details within the boundary layer, and moreover provide no evidence as to the shape of the boundary layer velocity profiles. These are essential both for the understanding of the fluid mechanisms involved and for possible inclusion within computational codes. Additionally many of the flow visualisation techniques are also susceptible to affecting the flow itself. China clay, invaluable in static tests, is also subject to centripetal forces and therefore suggests the flow to be moving in a more radial manner than is actually the case.

Considerable effort has been made to provide quantitative information on rotor boundary layers but with little success. The conventional method of traversing a hot-wire probe through the boundary layer of an aerofoil to determine the velocity profile becomes virtually impossible with the blade rotating. It is necessary to either embed the hot-wire probe within the rotating blade or to mount the probe

externally and allow it to rotate with the blade. Both techniques are inflexible, complex and highly intrusive. Additionally three-component information cannot be acquired.

The Laser Doppler Anemometer (LDA) has within the past two decades provided accurate velocity measurements in a variety of flows. The technique is non-intrusive as it is based upon small 'seeding' particles passing through a pair of intersecting laser beams at their focus and scattering light (the region of intersection is referred to as the measurement volume). As the measurement volume approaches any surface flare dominates over the light scattered by the seeding particles, eventually to such an extent that there are no validated bursts. With LDA measurements on a rotor these problems occur, though only as the blade rotates either near or through the measurement volume, and therefore only periodically. It is primarily this periodic increase in flare which has rendered previous attempts unsuccessful.

A reduction in the flare was consequently of prime concern, but further improvements to the operation of the LDA would also be required. A model helicopter rotor operating in hover was used as it provided a simple flow with a small hub and large aspect ratio - ideal for verification of Himmelskamp's postulate. Evidence from two distinct flow visualisation studies helped form the LDA test program. This covered a range of pitch angles and rotational speeds, though aerodynamic conclusions were never a prime concern. The aim was rather to develop techniques which could in the future be employed in a comprehensive test program.

Flow Visualisation Tests

The tests were all carried out within a large, dedicated, area. The rotor blades (chord 0.062m, semi-span 0.8m), of Gottingen 436 section, were from an ML Aviation Sprite, a remotely piloted vehicle employing two contra-rotating coaxial, two-bladed rotors. Two 3mm bore plastic tubes were inserted, at 5% and 40% chord (Fig. 1), reaching from the root to the tip. For these tests the two-bladed rotor, mounted on a teetering hub, was driven by a 3KW electric motor - a Sami-Ministar frequency converter allowed control of the speed to better than 0.033%. Results were taken at four pitch angles (1, 6, 11, and 16 degrees), and four rotational speeds (200, 400, 600, and 800 RPM) corresponding to a maximum Reynolds number, based on chord, of 400,000.

Two different flow-visualisation techniques were initially employed to establish the regions which might benefit the most from study by LDA. The first flow-visualisation technique, first documented in Ref. 2 and Ref. 3, involved injecting ammonia into the boundary layer and observing the subsequent discolouration of a suitable surface reagent (Fig. 2). In practical terms it was achieved by allowing ammonia vapour from a container at the rotor hub to pass down a delivery tube connected to either the 5% or 40% chord tubes, sealed at the tip. A series of 0.65mm diameter holes staggered along the tubes and reaching to the surface enabled the ammonia to escape and become entrained into the boundary layer flow. The ammonia then reacted with a thin blueprint film affixed to the blade to reveal narrow but distinct streaks.

The results showed discontinuities in the traces which were attributed to standing laminar separation bubbles (Fig. 3). This is in agreement with a similar series of tests described in Ref. 4. The discontinuities were seen to move forward and shorten with increased pitch angle and Reynolds number. It was concluded that the stall, which only occurred at the outboard stations, was of the leading edge type, with the mechanism being the bursting of the bubble. Results immediate to the hub were little different to those at other inboard stations and therefore the hub was not considered an important factor in the existence of the radial flows. Radial flows were found to be particularly prevalent within the separation bubbles, though there was some evidence of radial flow both within other regions of separated flow and within turbulent boundary layers near the trailing edge. The actual strengths of these radial flows relative to the chordwise flow could however not be ascertained as the results were purely qualitative. Overall the results showed that this rotor operating in hover provided a suitable test for the LDA, and that a comparison between an inboard and an outboard station would be of particular interest.

The second flow-visualisation technique involved the adaptation of a laser light sheet to provide streamlines in a plane perpendicular to a given chordwise section through the Gottingen 436 blade. The technique, derived from an idea proposed by Duncan and Collar (Ref. 5), solved the problem of ensuring

that the flow should be measured relative to the blade, ie. that to a stationary camera the blade should appear stationary - the alternative solution of rotating the camera with the blade is problematic. As shown in Fig. 4 the technique involved affixing two mirrors back-to-back at the centre of rotation and through suitable gearing allowing them to rotate at half the rotational speed of the blade. With a camera focused to the image of the blade on the front plane of one of the mirrors, the blade, though rotating, appears stationary.

In total darkness, but with a single laser beam directed vertically from above the plane of rotation and at a radial position to which the camera, observing the image of the blade in the mirror, has been focused the camera shutter is opened some time before the passage of the blade through the laser beam. As the blade passes through the beam it, and any smoke moving relative to it, is illuminated. When integrated over the total blade passage through the laser beam the combined image is as if the blade were illuminated by a light sheet but of a much higher light intensity. The alternative solution of employing a much more powerful laser would have proved prohibitively expensive, and unsafe. The technique proved successful but the results were disappointing due to the difficulty in ensuring a sufficient quantity, and especially uniform distribution, of smoke - a problem equally applicable to the LDA. In addition the results showed some vertical motion of the blade relative to the plane of revolution, which would have to be solved prior to any LDA tests.

Introduction to the LDA

In its simplest form an LDA consists of a source of laser light, producing a single beam, which is then divided into two beams of equal intensity (Fig. 5). Passed through a lens these beams are then focused to a common point, known as the measurement volume. Micron sized particles inseeded into the flow pass through this measurement volume scattering light. The scattered light is then collected through receiving optics and converted to an electric signal by a photomultiplier. Finally the frequency of the oscillations present within this signal is determined. It is this 'Doppler' frequency which is proportional to the speed of the seeding particles through the measurement volume and therefore to the flow itself.

For the department's three component Dantec LDA the same principles apply. In this case there are however three such pairs of beams all aligned to the same position in space, and therefore for a given seeding particle three Doppler frequencies to be determined. Fig. 6 shows a schematic of the LDA. The core part of the system is a high precision, fully automated, 3-axis Dantec traverse, which is able to survey a region of 0.6m x 0.6m x 0.6m. On an optic bench affixed to the traverse two long-throw optic heads (focal length 1600mm) can be mounted in a number of different configurations. Two pairs of orthogonal beams (green and blue) are emitted from one of the optic heads (2D) and a third pair (violet) from a second optic head (1D). Both optic heads, able to receive as well as transmit light, are linked to a beam-splitter unit by 10m fibre-optic cables. This unit acts as the interface between the laser source (5 Watt Spectra-Physics Stabilite laser) and the fibre-optic cables. Its purpose is to provide, from the single beam emitted by the laser, the required three pairs of beams of different wavelength (green, blue, and violet). A Bragg cell removes any problems of directional ambiguity. Processing to obtain the Doppler frequency is in this case performed by three Burst Spectrum Analysers (BSAs), since upgraded to Enhanced BSAs. A software suite comprises routines for automated data acquisition, data processing and graphical presentation.

Description of Technique

Initial Limitations

With the LDA traverse positioned as far as possible from the centre of rotation the beams are aligned to the required radial position, and in approximately the plane of rotation. The azimuthal position of the measurements is chosen to be that when the rotor blade passes closest to the LDA traverse, thereby, as is shown in Fig. 7, minimising any interference to the flow.

With the LDA set to acquire data continuously a frequency, and hence velocity, measurement is obtained for each seeding particle as it passes through the measurement volume. With the arrival time for each individual seeding particle also being determined the result is a scatter distribution of velocity

against time (Fig. 8 shows the scatter distribution over one cycle). To increase the number of velocity realisations per blade revolution a once-per-revolution encoder was added. This enabled the velocity information over a number of cycles to be collated, from which each velocity realisation could be sorted into time relative to the start of each revolution. The technique is known as rotor sampling, the result of which is shown in Fig. 9. The scatter distribution can then be divided into either time and hence azimuthal bins, within which mean and turbulence information can be determined. In order to provide a sufficient sample size within each azimuthal bin and to ensure that each bin was of a similar size to the measurement volume, that is 0.1mm in diameter, a substantial amount of data was required. Evidently the data rate, defined as the number of validated velocity samples per second, had to be increased substantially.

The second, fundamental, problem occurred when the rotor blade passed through, or very near, the measurement volume. Where boundary layer data would have been expected, no such data was apparent. This problem of flare swamping genuine signals is common to all LDAs. A number of solutions to the problem exist, but experience has shown that the best method lies in collecting light off-axis rather than in direct backscatter. In this mode light from seeding particles passing through the measurement volume created by a pair of beams from one optic head is collected by the opposing head mounted alongside. The measurement volume as a result of collecting light off-axis is significantly smaller than that achieved when collecting in direct backscatter, ie. through the emitting optic head. It is effectively spherical rather than ellipsoidal. However, it is also known that according to Mie Scattering theory (Ref. 6) there is at least an order of magnitude less light scattered in the off-axis direction than in the back-scatter direction. The data rate, already too low, would be significantly reduced. A further reduction in data rate exists due to fewer seeding particles passing through the small, off-axis, measurement volume in a given time than through the large, back-scatter, measurement volume.

This constant trade-off between high data rate and both reduced flare and improved spatial resolution was finally solved by the development of an improved method of aligning the laser beams to a common focus. This alignment is a pre-requisite for any LDA system, but the limited amount of literature available on the subject *incorrectly* implies that for many systems or tests good alignment is not critical. Subsequent studies within the department have shown improving the alignment to be the single biggest improvement which can be made to a given system.

Alignment Procedure

The conventional method for Bristol's LDA was to divert a small amount of light down each of the two collection fibres in turn (Fig. 10). This illuminates a conical region, the 'base' of which is the front lens and the measurement volume its 'apex'. This is in effect the path taken by the light scattered as seeding particles pass through the measurement volume. The images created on a back-screen by these conical regions as they are focused through a 50mm focal length lens are then observed. As the size of the image on the back-screen reaches a minimum the conical region is deemed to be focused (Fig. 11). The process is repeated for the second conical region, ie. for light passed down the collection fibres of the second optic head. Attention is then turned to the individual laser beams. The beams are assumed to be correctly aligned when, with no light diverted down the collection fibres, their images on the back-screen are concentric. Small adjustments can be made to the beams emitted from the optic head as necessary. Inevitably the level of success was controlled by the ability to successfully identify and make adjustments to the concentricity and size of the images. As such the method was seriously flawed.

The improved alignment technique depends on the much more mechanical process of observing the output of a light dependent resistor mounted behind a 20 micron diameter pinhole (Ref. 8, Ref. 9). As with the conventional alignment technique described above light is directed down each collection fibre in turn. The focus can be readily discerned on the front face of the pinhole surround (Fig. 12). By then traversing in a vertical and lateral direction the focus can then be aligned to the pin-hole. A minimum reading on the light dependent resistor then corresponds to a maximum amount of light passing into the pin-hole and hence an optimum alignment relative to the pin-hole. The process is then repeated for the second conical region, ie. for light passed down the collection fibre of the second optic head. With no light passed down the collection fibres each beam is then in turn aligned to the front face of a pin-hole. As the light intensity distribution across a laser beam is essentially Gaussian a minimum reading corresponds to the exact centre of the beam being located at the pinhole. Repeating this for each of the six

beams in turn completes the alignment process. Only forty five minutes are generally required and the success rate is better than 95%.

To summarise therefore, the pin-hole alignment procedure guarantees the ability to collect light off-axis and with a very high data rate. The subsequent benefits of the former lie in reduced effects of flare on genuine signals, and in a spherical rather than ellipsoidal measurement volume. For these rotor tests the benefit of collecting light off-axis is demonstrated by the comparison of the scatter distributions of velocity against azimuthal position, Fig. 13, for the back-scatter and the off-axis modes. It is only in the latter that any measurements within the boundary layer are possible. In addition the data rate increased by an order of magnitude, which further demonstrates the importance of good alignment.

LDA Settings

In a steady flow, with a steady throughput of seeding through the measurement volume, increasing the processor gain and photomultiplier high voltage improves the signal to noise ratio and hence the data rate. Eventually the noise within the signal dominates to a greater extent and the data rate decreases. The data rate display on the front of the BSAs enables the optimum amplification levels to be set. However, for the rotor tests neither the flow, nor the throughput of seeding, are constant enough for the effect of changes in amplification levels to be analysed. In addition flare dominates over the signal twice every revolution. The final difference is that only a portion of every cycle is of interest, ie. only when the measurement volume is within or close to the boundary layer. The optimum data rate must therefore be set for this limited portion, rather than for the entire flow.

The solution was to acquire data for a fixed period of time, and for a number of different combinations of processor gain and photomultiplier high voltage, process the data and observe either the scatter distributions of velocity against azimuthal position or the probability density functions of velocity. Fig. 14 reveals that at the lowest amplification levels (gain of 20) there is a single, narrow, velocity peak. This corresponds to the blade passing through the measurement volume. At this amplification level the light intensity caused by the genuine seeding particles scattering light does not exceed the required threshold value. As the amplification level increases (gain of 30 or 40) the intensity of the signals from genuine seeding particles does exceed the threshold value and the result is a much greater distribution of velocity corresponding to an increased proportion of measurements being acquired with the measurement volume within the boundary layer and not being adversely affected to too great an extent by flare. As the processor gain reaches 50 however increased noise is introduced and the proportion of 'boundary layer data' decreases. This technique of maximising the distribution of velocities therefore enables the optimum amplification levels to be set.

Even at the optimum amplification levels there still remains some 'data' from the blade itself. Indeed it is only through determination of their relative transit times, that is the length of time for which the signals exceed the threshold value, that the genuine data can be separated. For the same velocity 'data' from the blade passing through the measurement volume has significantly higher transit times, and this forms the basis for their rejection. Fig. 15 shows the value of this data rejection criterion in the removal of erroneous data.

Variations in Blade Height

Acquiring data simply with the rotating blade varying in vertical position relative to the plane of rotation would have led to the boundary layer velocity profiles being elongated. Rather than employing a rigid blade data was therefore only acquired when the blade passed at a known height relative to the plane of rotation. This was achieved by positioning a 5mW Helium-Neon laser alongside the LDA traverse, a thin fibre-optic cable within the 5% chord tube used for the flow visualisation tests described above, and a light dependent diode mounted at the hub. When light of a sufficient intensity from the 5mW laser, aimed at the blade tip just prior to its passage through the measurement volume, is received by the diode an enabling signal is sent to the BSAs. It is therefore only when the blade is at a certain height relative to the plane of rotation that light passes down the fibre optic and data is acquired. Through the use of optical filters this technique provides a resolution in blade position of 0.01mm. A schematic showing the principles is shown in Fig. 16. The enabling signal to the BSAs additionally acts as the once-per-revolution encoder signal to the master BSA. To reduce the amount of data collected the BSAs were also

only enabled for a period corresponding to the time required for the passage of the blade through the measurement volume. The technique is referred to as strobing.

A by-product of this technique is that it provides a unique and highly accurate method of tracking rotor blades. Small variations in the pitch angle of the rotor blade within which the fibre-optic cable was mounted radically changed the proportion of revolutions over which sufficient light was received by the laser diode. Monitoring this proportion of validated signals and 'tweaking' the pitch angle, improved the tracking by a considerable degree. The technique could readily be introduced into full scale rotors.

Frequency to Velocity Transformation

The frequencies determined by each pair of beams, and for a given seeding particle, have to be converted into velocities. This involves determining the corresponding calibration factor (Doppler frequency (MHz) to velocity (m/s)), which is dependent on the included angle between each pair of beams and on the wavelength of the beams in question. Finally these velocities which are exclusive for a given optical configuration have then to be converted into a global set of orthogonal values. This is determined directly from knowledge of the beam measurement vectors.

The required values for the calibration factor and the elements of the velocity transformation matrix are the result of the same procedure. The technique is based upon determining the coordinates of each of the six beams as they cross two distinct parallel planes a known distance apart (Ref. 7, Fig. 17). Conventionally this has been achieved by marking off the beam position on a board or photographic plate. However small errors can ensue which are then carried through to produce significant errors in the final orthogonal velocities. The pin-hole meter, as employed for the alignment procedure described above has therefore been adopted. By positioning the pin-hole meter at a suitable location and then using the traverse to position each beam, twice for the two planes, in turn at the pin-hole, using the output of the light dependent resistor, and noting the coordinates of the traverse as they appear in the software the coordinates for the centres of the beams can now be determined to a very high degree of accuracy. These are then substituted into a spreadsheet program to provide the elements of the transformation matrix and, with knowledge of the beam wavelengths, to provide the calibration factors.

Data Reduction

The ability to acquire accurate velocity data within the boundary layer of a rotor blade has been amply demonstrated by the scatter distribution of velocity against azimuthal position. However, to be of any value the data has to be transformed into boundary layer velocity profiles relative to the rotating blade. This required a number of stages. The first two, namely removal of data not fulfilling transit time requirements and binning of data according to azimuthal position, have already been covered. For each vertical position of the measurement volume relative to the plane of rotation the azimuthal positions of the first and last samples with excessively large transit times provides the location of the fore and aft of the blade as it passes through the measurement volume. This, for the 150 or so heights relative to the plane of rotation, enables the coordinates, in terms of azimuthal position, of the fore and aft location of the blade surface to be determined. This relates directly to the coordinates of the blade profile.

With the azimuthal location of the fore and aft positions of the blade surface determined, a combined file is generated to provide the orthogonal components of velocity (U, V, and W relative to the LDA traverse) in the form of a 2D grid surrounding the blade with gaps corresponding to the measurements 'within' the blade surface. The trailing edge is then defined as position (0, 0, 0) and all azimuthal positions converted into cartesian coordinates relative to this datum. At this stage all velocities are converted into values relative to the rotating blade and not relative to the traverse. This requires knowledge of the rotational speed and the radial position of the measurement volume.

Finally the velocities are converted from values relative to the rotating blade into values relative to the curved blade surface - a boundary layer velocity profile, to be of value, must be perpendicular to the local surface. Fig. 18 shows the principal stages.

Interpretation of Results

This work was carried out with the intention of developing suitable techniques rather than carrying out an extensive aerodynamic study into rotor boundary layer flows. In this case results were obtained at four pitch angles, four rotational speeds, and two radial stations.

Several characteristics are worthy of comment. Fig. 19 shows an intermediate case (6 degree pitch, 600 RPM and at an inboard station) with six boundary layer velocity profiles provided at equidistant positions along the chord. The first profile ($x/c=0.14$) is characteristic of a laminar boundary layer. The flow is nominally 2D, with a boundary layer thickness of 0.13mm. As the distance from the leading edge increases the adverse pressure gradient comes into effect with the slow moving air, nearest the surface, being the most strongly affected and hence most heavily retarded.

As x/c reaches 0.57 the strong adverse pressure gradient results in a region of reversed flow which, for a 2D static wing, is indicative of a laminar separation bubble. This is due to the laminar boundary layer separating, undergoing transition and then due to its greater energy reattaching further downstream as a turbulent boundary layer. Profiles characteristic of a turbulent boundary layer can be noted for the two most aft positions.

The results in Fig. 19 also help to quantify the extent of the spanwise flow. The strongest spanwise flows are noted within the separation bubble with values of up to 10.4% of the chordwise velocity. Within the turbulent boundary layer the spanwise flow again decreases. The hypothesis is consequently that significant spanwise velocities are only noted when the flow is separated and is able to be influenced by a combination of the spanwise pressure gradient, centripetal forces, and the Coriolis effect.

The results in Fig. 20 show that as the rotational speed, and hence Reynolds number, is increased the separation bubble moves forward and to some extent shortens. This is in agreement with the flow visualisation results described above, and can be ascribed to the boundary layer becoming more susceptible to pressure gradient effects. A similar trend is also observed as the pitch angle is increased, in this case due to an increased pressure gradient.

For the outboard stations similar results are obtained for the chordwise velocity profiles - again in agreement with those obtained from flow visualisation studies. However at the highest pitch angles and rotational speeds the spanwise velocity within the separation bubble is much reduced. It is possible that it is the effect of the tip vortex which counters the expected spanwise flow. Though confirmed by the flow visualisation results further studies are required.

Discussion of Potential Errors

The errors are fundamentally of three distinct forms and each will be discussed individually - an appraisal of their combined effect will then be given.

The conventional sources of error involved with Laser Doppler Anemometry apply. Through the use of the highest quality Dantec equipment, through the development of the pin-hole alignment technique, and through optimising the operation of the system these errors have been minimised. This maximises both the signal to noise ratio and the spatial resolution. However small, errors do still exist, and those that do are further accentuated by the conversion of the velocities into a global set of values. Again use of the pin-hole meter minimises such errors. All these sources of error have previously received significant attention, and by a number of authors.

The errors associated with the rotor rig are believed to be minimal. The technique does, however, require the state of the boundary layer to remain the same over the period of testing. Comparative data acquired at various stages during a test period has shown this to be the case.

It is in the conversion of the velocities from the scatter distributions against azimuthal position into boundary layer profiles relative to the rotating blade that the greatest sources of error are anticipated.

The process involved a significant degree of interpolation, and it is in this area that future work could benefit.

In conclusion it is accepted that there are a number of potential sources of error, most of which cannot be quantified. The trends shown in the boundary layer profiles are however genuine though the values themselves may be subject to a maximum 10% error. Further improvements, particularly in the post-processing of the data would be beneficial.

Conclusions

The improved understanding which 3D boundary layer velocity information could offer to rotating machinery has long been appreciated. Previous attempts at providing quantitative data within the boundary have however essentially failed. In this respect this paper has described how improvements in the use of a three component LDA have led to a unique series of boundary layer velocity profiles being determined on a helicopter rotor operating in hover. The principal breakthrough has been the development of a quantitative alignment technique which guarantees a much higher data rate, and greatly improved signal to noise ratio and spatial resolution. Methods of only acquiring data at a known position relative to the flapping blade and ensuring that the resultant data is genuine have also proved essential.

The resulting boundary layer velocity profiles have shown the existence of laminar separation bubbles, in agreement with results from two distinct flow visualisation studies. The spanwise flows which exist within the bubble can reach 10% of the chordwise velocity. Both the LDA tests and the flow visualisation studies have shown these laminar separation bubbles to both shorten and move forward with increased pitch angle and rotational speed. The effect of the rotor hub is minimal.

References

- 1) Himmelskamp, H. "Profiluntersuchungen an einem umlaufenden Propeller". PhD Thesis, Gottingen, 1945. [Profile Investigations on a Rotating Airscrew]
- 2) Ruden, P. "Turbulente Ausbreitung im Freistrah". Naturwissenschaften, 1937.
- 3) Johnson, J.P. "A Wall-trace, Flow Visualisation Technique for Rotating Surfaces in Air". ASME Journal of Basic Engineering, 1964.
- 4) Velkoff, H.R., Blaser, D.A., and Jones, K.M. "Boundary Layer Discontinuity on a Rotor Blade in Hover". AIAA Journal of Aircraft, Vol. 8, No. 2, 1971.
- 5) Duncan, J., and Collar, A.R. "Present Position of Investigation of Airscrews". Aeronautical Engineering Council, Reports and Memoranda No. 1518, Dec. 1932.
- 6) Drain, L.E. "The Laser Doppler Technique". Wiley and Sons Ltd., 1980.
- 7) Swales, C., Rickards, J., Brake, C., and Barrett, R.V. "Development of a Pin-hole Meter for Alignment of 3D Laser Doppler Anemometers". Dantec Information, Vol. 12, 1993.
- 8) Swales, C. "Advanced LDA Techniques for Measurement of 3D Boundary Layer Velocity Profiles on a Helicopter Rotor". PhD. Thesis, Department of Aerospace Engineering, University of Bristol.
- 9) Dewhurst, S.J. "Fluid Flow Studies Using Three Component Laser Doppler Anemometry". D. Phil, Thesis, Oxford, 1993.

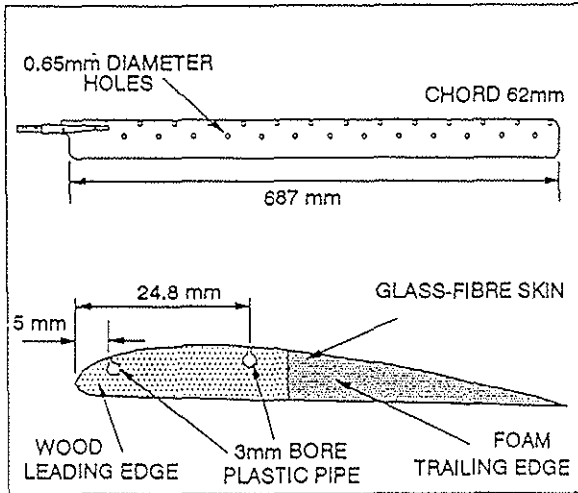


Fig.1 Gottingen 436 Blades

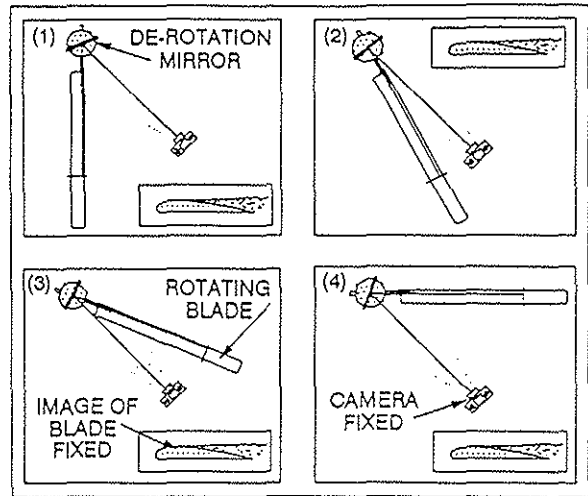


Fig.4 Principle of De-rotation Mirror

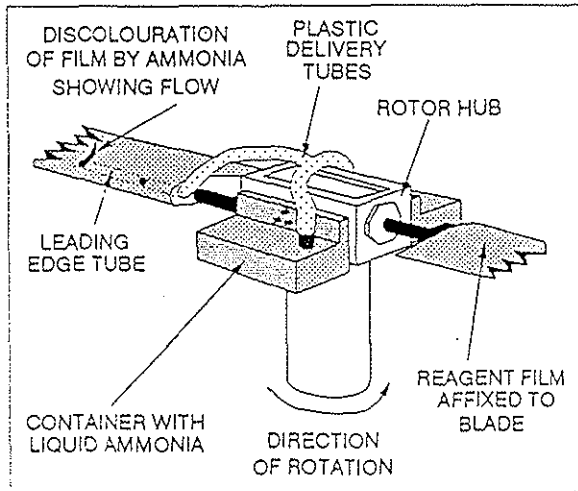


Fig.2 Injection of Ammonia Vapour Into Boundary Layer

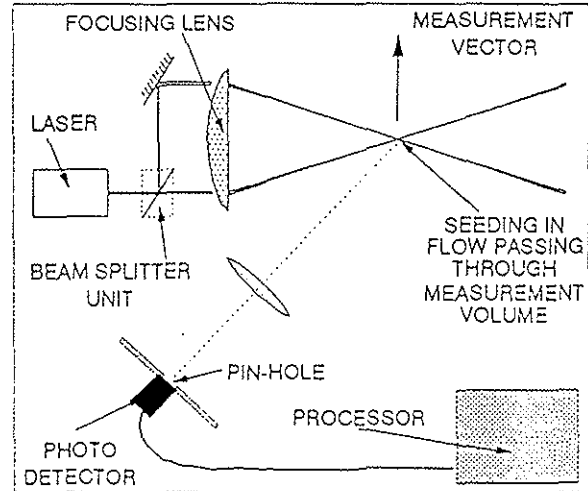


Fig.5 Principles of Laser Anemometry

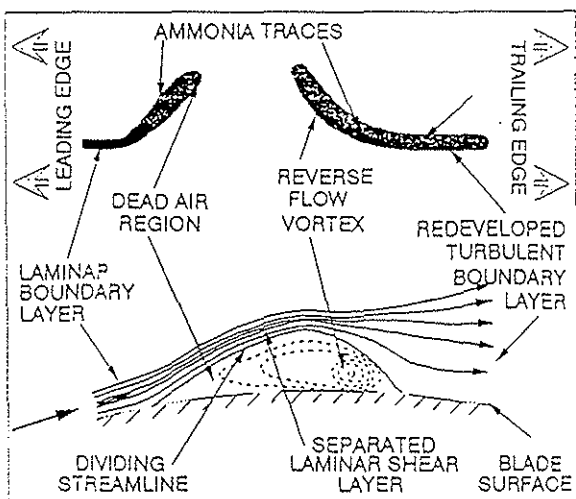


Fig.3 Explanation for Discontinuities in Ammonia Traces

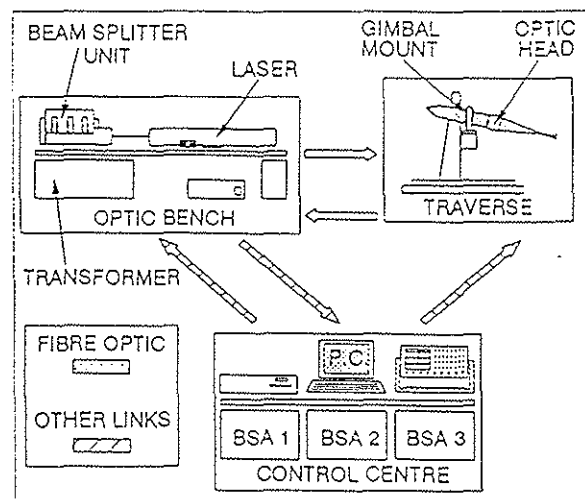


Fig.6 Schematic of LDA

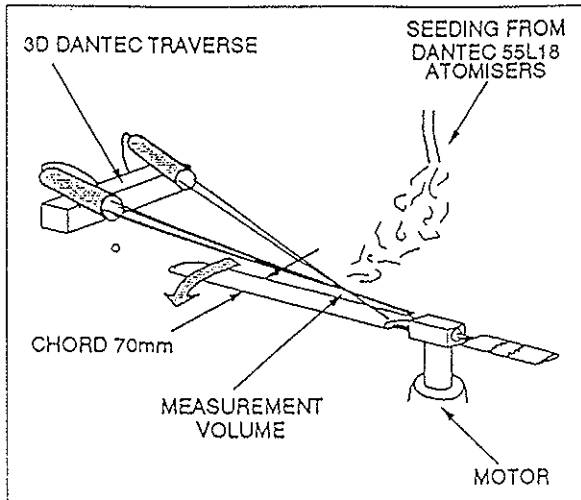


Fig.7 Position of LDA Relative to Rotor

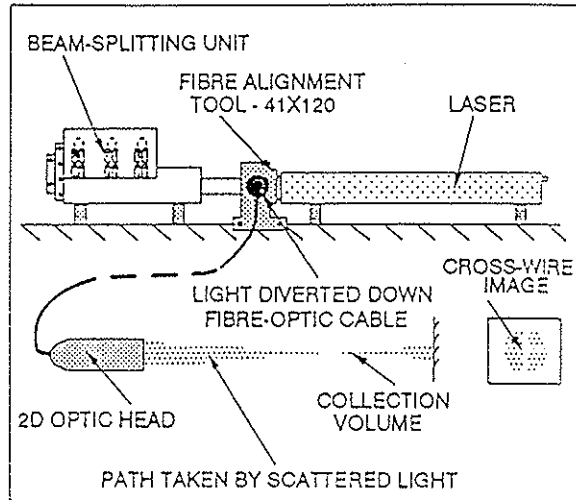


Fig.10 Making Collection Volume Visible

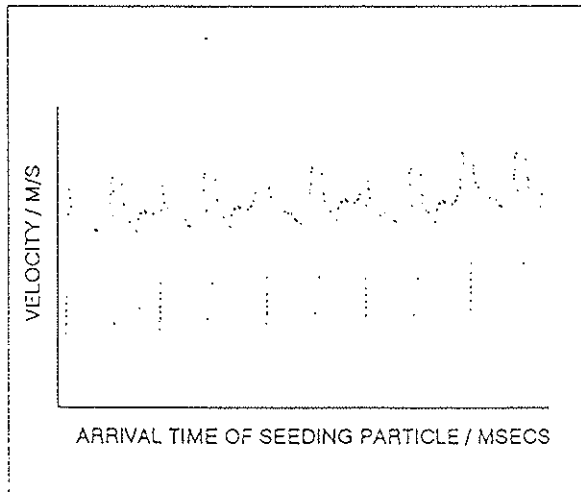


Fig.8 Velocity Against Time - No Encoder

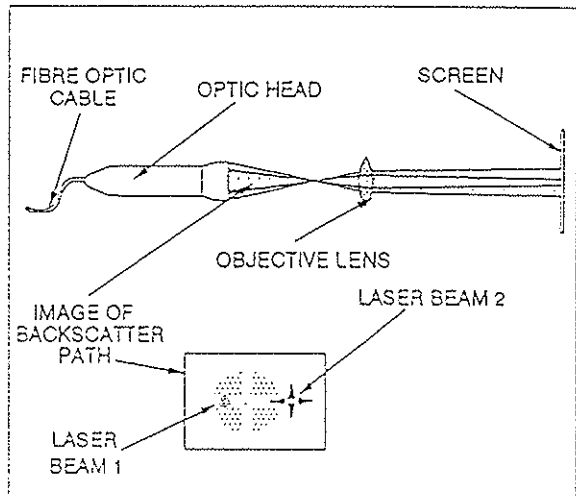


Fig.11 Conventional Alignment Technique

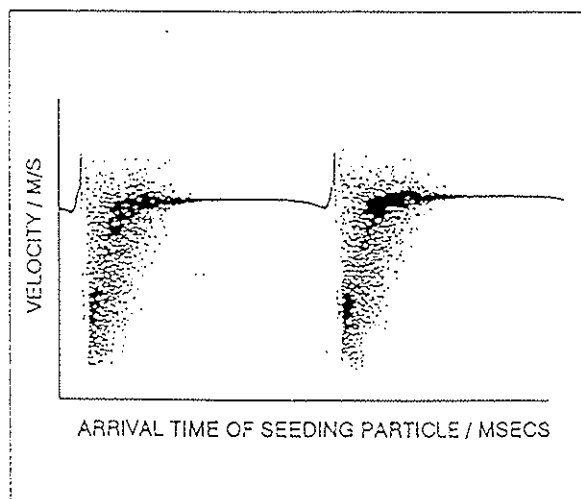


Fig.9 Velocity Against Time - Encoder

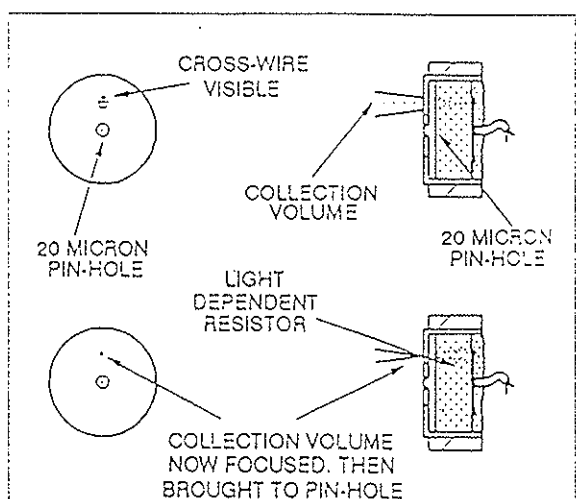


Fig.12 Pin-hole Meter Alignment Technique

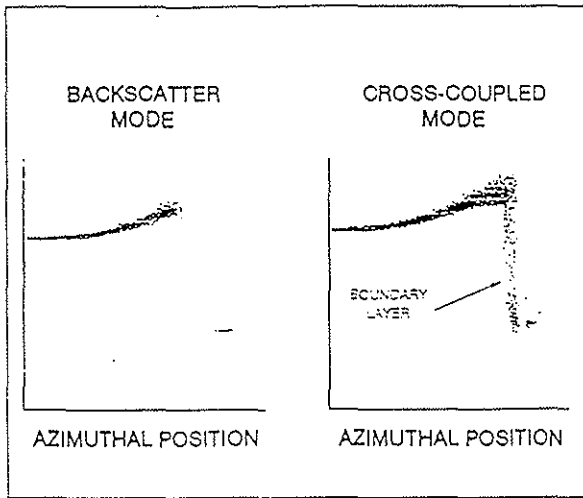


Fig.13 Effect of Mode of Operation

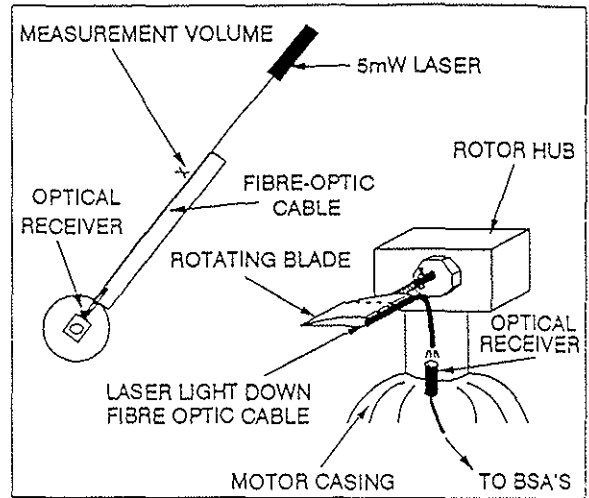


Fig.16 Conditional Blade Height Sampling

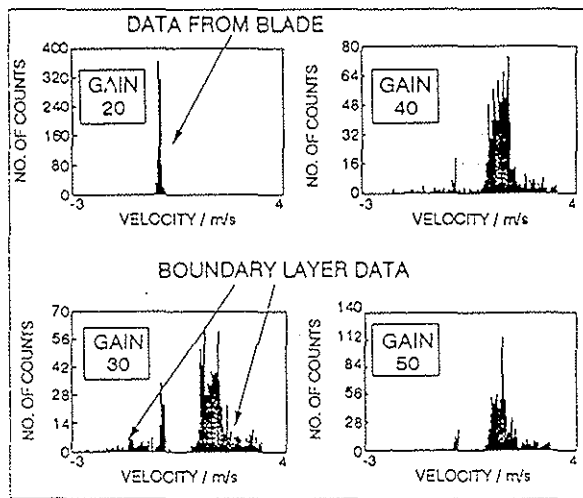


Fig.14 Effect on Velocity as Gain Increases

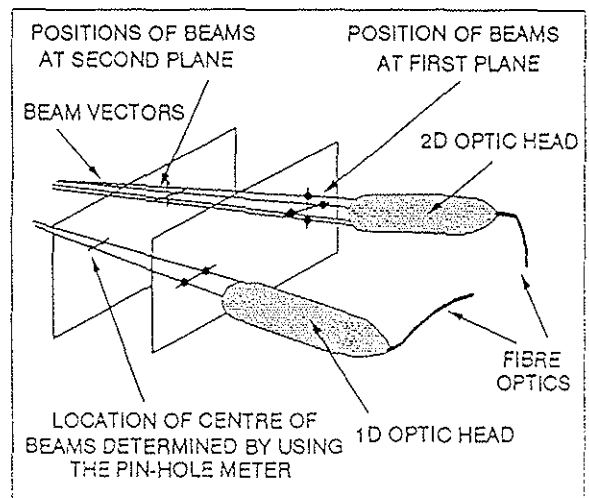


Fig.17 Determination of Transformation Matrix

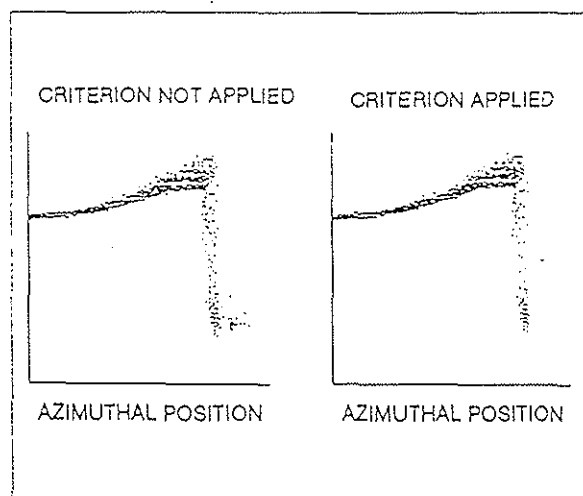


Fig.15 Effect of Transit Time Rejection

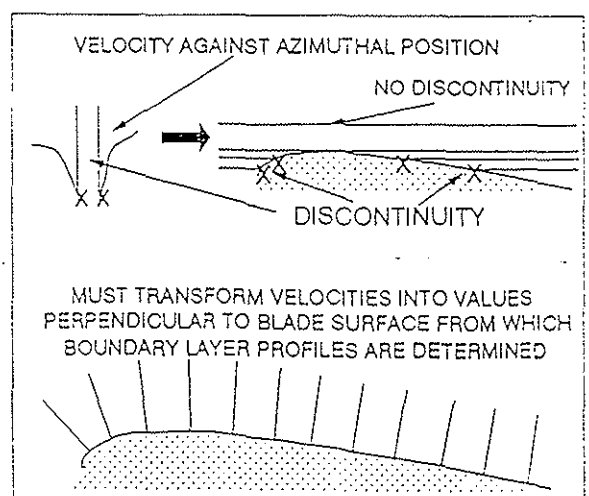


Fig.18 Schematic of Data Reduction

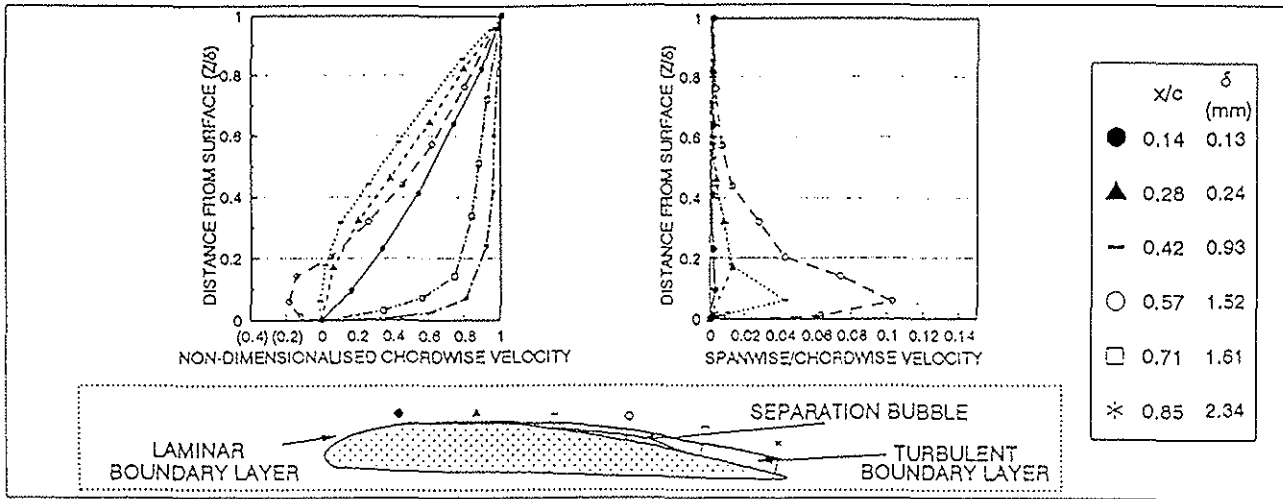


Fig.19 Example of 3D Boundary Layer Velocity Profiles (600RPM, 6 Degree Pitch) (Inboard Station)

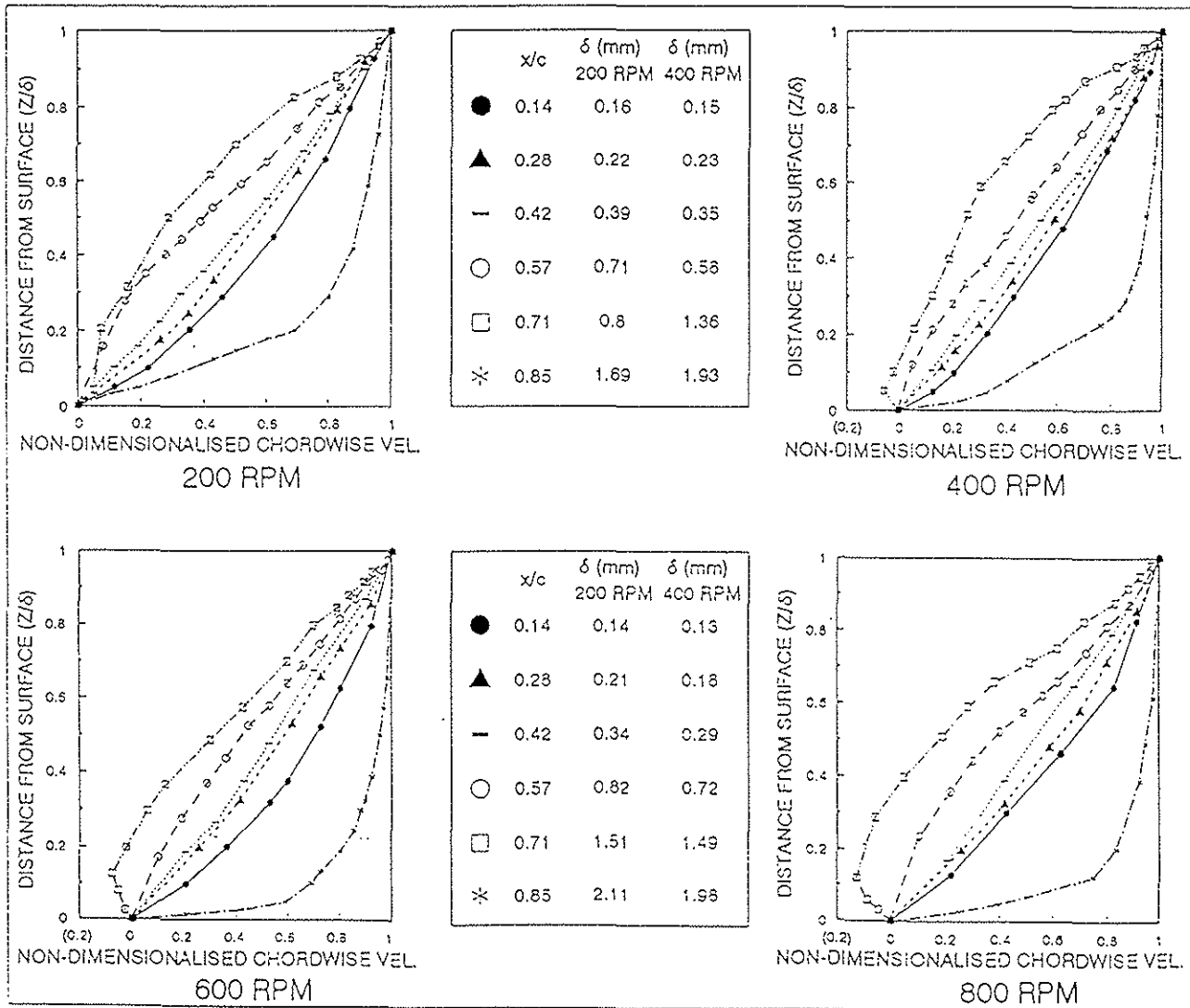


Fig.20 Effect of Increase in Rotational Speed on Boundary Layer Profiles (1 Degree Pitch, Inboard)